



HAL
open science

Investigations on solidification and fluid flows during GTA welding with in-situ observations

Alexis Chiocca, Cyril Bordreuil, Fabien Soulié, Frédéric Deschaux-Beaume

► **To cite this version:**

Alexis Chiocca, Cyril Bordreuil, Fabien Soulié, Frédéric Deschaux-Beaume. Investigations on solidification and fluid flows during GTA welding with in-situ observations. 9th international conference of young scientists on welding and related technologies, May 2017, Kyiv, Ukraine. hal-01902725

HAL Id: hal-01902725

<https://hal.science/hal-01902725>

Submitted on 23 Oct 2018

HAL is a multi-disciplinary open access archive for the deposit and dissemination of scientific research documents, whether they are published or not. The documents may come from teaching and research institutions in France or abroad, or from public or private research centers.

L'archive ouverte pluridisciplinaire **HAL**, est destinée au dépôt et à la diffusion de documents scientifiques de niveau recherche, publiés ou non, émanant des établissements d'enseignement et de recherche français ou étrangers, des laboratoires publics ou privés.

INVESTIGATIONS ON SOLIDIFICATION AND FLUID FLOWS DURING GTA WELDING WITH IN-SITU OBSERVATIONS

Alexis Chiocca, Cyril Bordreuil, Fabien Soulié, Frédéric Deschaux-Beaume

*LMGC, Univ. Montpellier, CNRS, Montpellier, France
e-mail: a.chiocca@isgroupe.com*

Abstract. The relation between fluid flows, solidification mechanisms and welding parameters during GTA welding of a Cu30Ni plate is investigated. An experimental study, based on in-situ observations of the trailing edge of a fully penetrated weld pool is carried out. The experimental setup includes: (i) a high-speed camera used to observe the solidification front and the fluid flow at microscale, (ii) two cameras placed over and below the plate used to observe the entire weld pool on the top side and back side respectively (iii) and an infrared camera used to monitor the temperature field on the back side. All these observation devices are employed to do measurements that allow us to explore and better understand the influences of the welding parameters on the solidification and the fluid flow behaviours, as well as between the different physical phenomena being involved.

Key words: GTAW, welding, solidification, fluid flow, in-situ observation, high-speed camera.

1. INTRODUCTION

The progress in welding technology and knowledge is in constant development. Nevertheless, it does not completely allow the control of the weld beads final microstructures. It is still difficult to obtain a microstructure that fits the required mechanical properties, without any defects such as centre line grain boundaries [1], porosities or inclusions [2]. Consequently, the solidification during welding is a complex phenomenon that needs to be investigated very carefully, in order to obtain the desired microstructure. During welding, the solidification conditions are very specific, because it is a rapid solidification regime, which is determined by high solidification rate, high thermal gradients and strong fluid flows in the weld pool.

The physical phenomena that control the solidification process have to be analysed on two scales. At macroscale (the scale of the weld pool), the solidification conditions changes along the solidification front, making the microstructure different from fusion line to centre line [3]. At microscale, the temperature conditions and the fluid flows have clearly a strong influence on the solidification process, by modifying the dendritic growth mechanisms [4–7].

The solidification front morphology is mainly influenced by the thermal conditions and the solidification rate imposed by the process characteristics [8]. The value of the ratio of the thermal gradient over the solidification rate gradually

modifies the shape of the solidification front, from planar to cellular, columnar dendritic, and finally equiaxed dendritic. In addition, the product between the thermal gradient and the solidification rate has a role on the dendrites arms sizes and spacing. The presence of fluid flow has also been found to have a determinant impact on the solidification behaviour. Several studies show a modification in the solidification rate and direction with the intensity and the direction of the fluid flow close to the front. The flow alters the heat and solute exchanges around dendrites, which changes the growth conditions of the dendrites [4, 5, 7].

From the trailing edge of the weld pool to the fusion line, it is well known that solidification rate decreases and thermal gradient increases, producing changes in microstructure, such as morphology transitions [2]. At this scale, the fluid flow is known to influence the shape of the weld pool [2, 9].

By the use of in-situ observations and measurements on two scales, the present paper aims at better understand the link between physical phenomena occurring in the weld pool and feed the literature with experimental data.

2. EXPERIMENTAL SETUP

An experimental setup has been designed to investigate physical phenomena on the two scales. It is an upgrade of a setup, detailed in a previous publication [10], which includes a moving

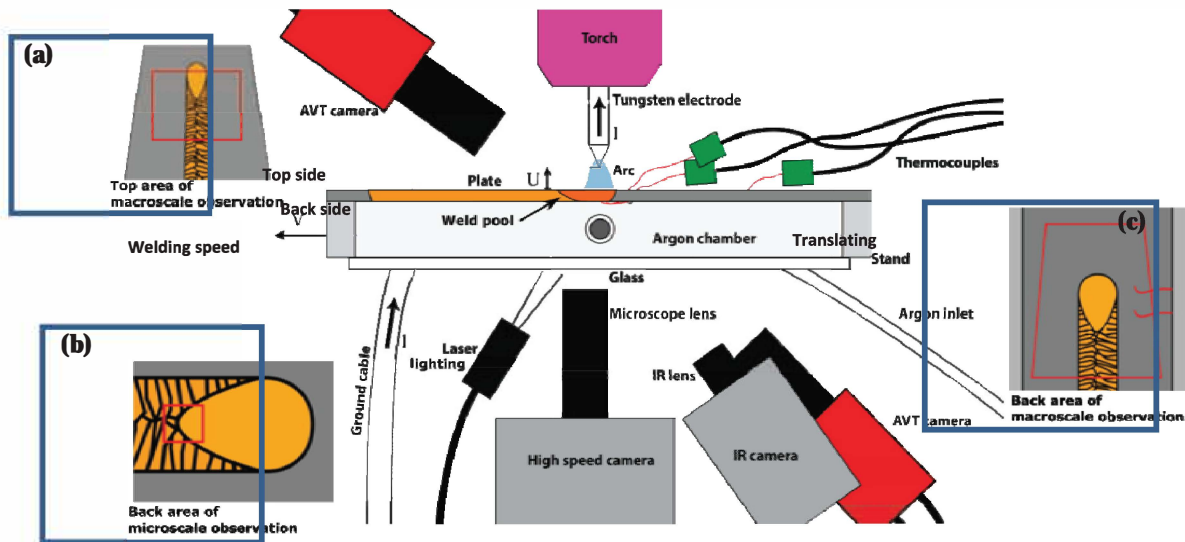


Fig. 1. Illustration of the experimental setup. Red framed areas at (a), (b) and (c) represent respectively the observation areas of the top AVT camera, the high-speed camera and the back IR and AVT cameras

stand (Fig. 1). A GTAW torch generates a fully penetrated weld pool on a 1.6 mm thick plate of Cu30Ni. The plate dimensions are $150 \times 70 \text{ mm}^2$ and the weld lines produced by the translation of the stand are 10 cm long. The two sides of the plate are protected by pure argon gas. The tests have been carried out with tungsten electrodes enriched with 2% of lanthanide, of a 1.6 mm diameter and a 30° grinding angle. The welding parameters have been chosen to obtain several set parameters filling the condition of a fully penetrated weld pool, without any collapse of liquid. The weld pool is only maintained by the surface tension. The welding parameters have been monitored using a voltmeter and a LEM and are referenced in Table 1.

The macroscopic observations of the fluid flow and the weld pool shape are made by two AVT cameras. They are filming in visible light the back side and the top side of the weld pool (in red on Figure 1). The temperature field in the solid part of the plate around the solidification front is measured on the back side of the sample thanks to an infrared camera. The thermal calibration of

the images of this camera is made with the help of two thermocouples placed in the base metal on the back side of the plate. A third thermocouple is monitoring the temperature of the stand. During tests, the microscopic observation is made on the back side at the trailing edge of the weld pool by a high-speed camera (5000 fps) and a microscope lens. The different observation areas are red framed on Figure 1 (a, b, c). All the measurements are synchronised in time.

All the methods used to process the different videos and extract the key measurements (thermal gradient, solidification rate and fluid flow) are described in detail in a previous publication [10].

3. RESULTS

At the macroscale, the combination of the thermal and visible observations on the back side allows the measurements of the thermal gradient and the solidification rate along the solidification front, from the trailing edge to the fusion line. As it is expected from the theory, the measured thermal gradient increases and the measured solidification rate decreases between these two points for the

Table 1. Welding parameters used for the tests (mean values)

Test	Heat Input, J/mm	Welding speed, mm/s	Voltage, V	Current, A
1	285	3	9.3	92.5
2	219	3	8.5	77.3
3	202	4.3	9.4	92.6

Table 2. Geometrical and thermal measurements at macroscale (mean values)

Test	Trailing edge gradient, K/mm	Fusion line gradient, K/mm	Top width, mm	Back width, mm	Back length, mm
1	105	278	8.3	8.0	15.2
2	100	245	5.4	4.5	8.1
3	109	196	5.8	5.1	11.9

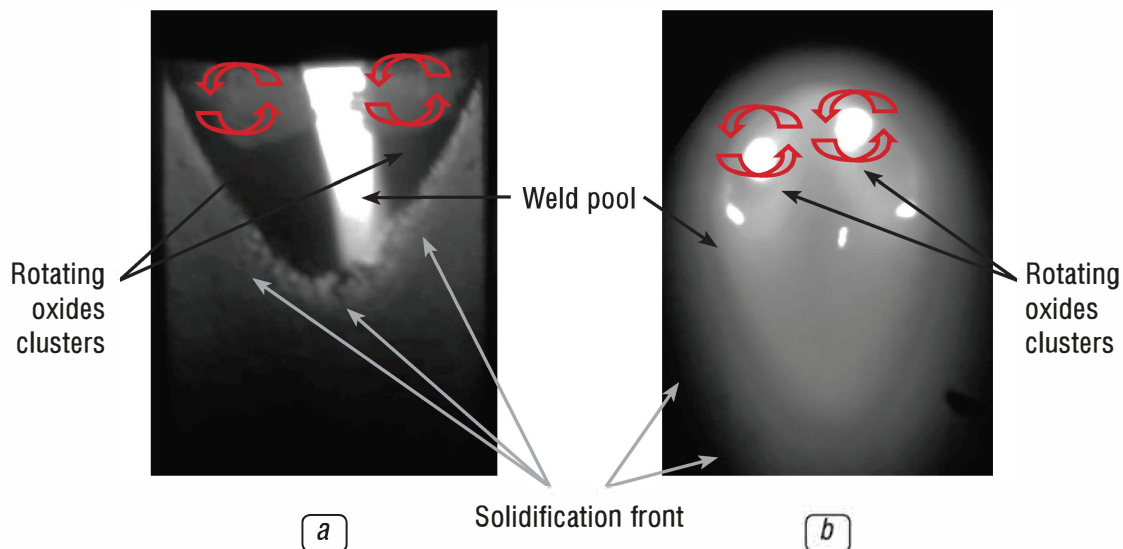
three tests. The shape modifications of the weld pools between tests are also in accordance with the theory. A higher welding speed (between tests 1 and 3) produces a longer and narrower weld pool and a lower current (between tests 1 and 2) produces a shorter and narrower one (Table 2). At the trailing edge the thermal gradient is rather similar between tests 1, 2 and 3, while the increase of the welding speed between tests 1 and 3 and the increase of the current between tests 1 and 2 should lead to a lower thermal gradient. The parameters should probably be changed in a larger range to obtain significant differences in thermal gradient measurements. Meanwhile, the reduction of the heat input seems to reduce the thermal gradient at the fusion line. This could be caused by a lesser temperature homogenisation of the weld pool, due to lower fluid flows when the heat input decreases.

At the macroscale, the observation of fluid flows revealed rotational movements. On Figure 2, the images extracted from the videos on the top side and back side show the symmetrical rotations of two oxides clusters on both sides of the weld

pool in the same direction. This could reveal the occurrence of a fluid flow going from the front centre of the weld pool to the trailing edge, following the centre line of the weld. Then, this flow seems to go back to the front by the edges of the weld pool, producing circulation.

The observation of the solidification front at microscale shows several phenomena. The dendritic growth at the trailing edge can be visible in-situ during welding on Figure 3a. On the left part of this figure, the primary dendritic arms growing into the weld pool are observed. This part is not homogeneous, it is fully or quasi solid on the left bottom corner, but by reaching the weld pool, in the semi-solid region the liquid part becomes more and more important. Between the results of the three welding parameters, no significant differences have been found on the inter-dendritic spacing or size of the semi-solid area. The only noted difference was the shape of trailing edge that is correlated with macroscale observations on the back side.

Thanks to little oxide particles, the fluid flows have been observed at microscale with a

**Fig. 2.** (a) top view of the weld pool, (b) bottom view of the weld pool

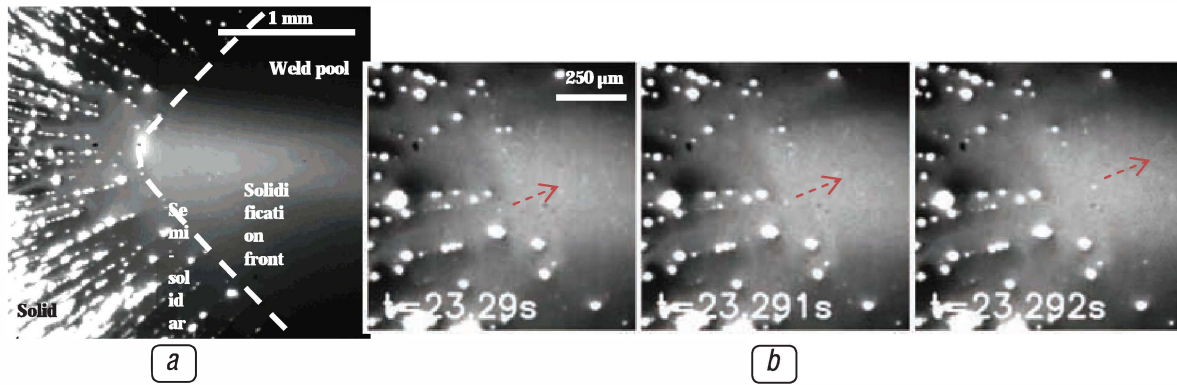


Fig. 3. (a) microscale view of the trailing edge of the weld pool, (b) three images taken every millisecond of the semi-solid area showing the displacement of particles

good accuracy (Stokes numbers calculated are around 0.1). The particles are seen appearing in liquid channels between primary dendrite arms, flowing from the root of the semi-solid area to reach the entirely liquid weld pool (Fig. 3b). The trajectories of these particles suggest the presence of a fluid flow in the semi-solid region. The measurements of the velocity of these particles by PTV (Particle Tracking Velocity [10]) show an evolution between the root of the liquid channels and the liquid pool. The curves on Figure 4a reveal that the fluid flow velocity is low (between 60 and 100 mm/s) in the channels. When the particles reach the limit of the semi-solid area (solidification front), they are accelerated to a higher velocity (between 110 and 180 mm/s). This implies that there are two different fluid circulations near the trailing edge of the weld pool (Fig. 4b): one flow into the liquid pool going from the top side trailing edge of the weld pool to the back side, and another flow following the same direction but crossing the semi-solid region.

Between test 2 and the two other tests, the flow velocity evolutions into the weld pool are different (Fig. 4a). The velocities are rather equivalent in the semi-solid region, but the fluid acceleration is more important after the solidification front, for test 2. This result seems surprising since it is generally considered that the flows in the weld pool are governed mainly by the Marangoni effect (surface tension gradient due to the temperature gradient on the surface of the weld pool), which increases with the heat input, whereas test 2 is not the one carried out at the highest heat input. However, the weld pools of tests 1 and 3 have sharper trailing edge than test 2 (Table 2), which can produce a fluid flow deceleration at the trailing edge, that is less important for test 2, due to the more rounded shape of the trailing edge.

Figure 4b shows schematically, on a longitudinal section, the rotating clusters observed in the weld pool at macroscale (Fig. 2). The rotation of the clusters occurs in the same direction on the top side and back side of the weld pool.

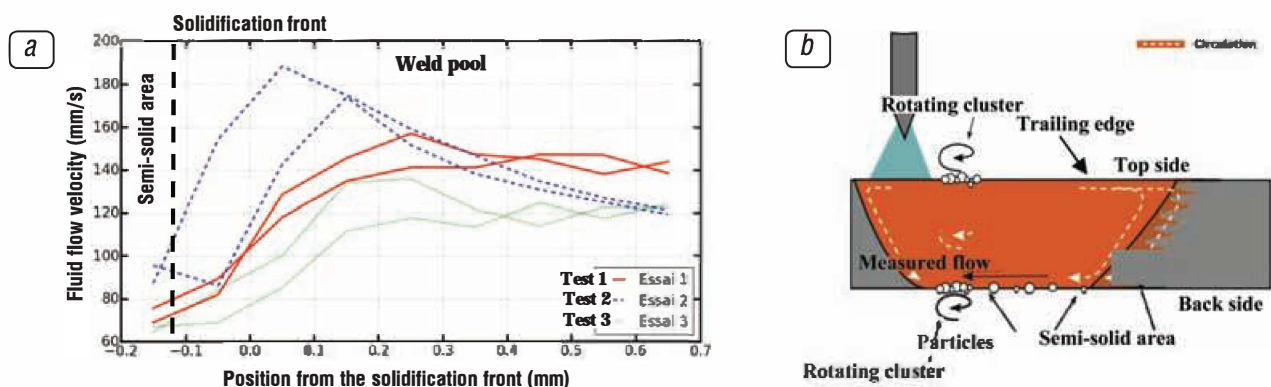


Fig. 4. (a) flow velocity evolutions from the semi-solid region to the weld pool for the three welding parameters (the 0 origin is the solidification front limit), (b) schematic representation of fluid flows in a longitudinal section of the weld pool during welding

It can be supposed that the rotations are present in the whole thickness of the weld pool as it is represented on Figure 4b.

Reynolds numbers have been calculated between the primary dendrites arms and in the liquid pool using data measured at microscale. Whatever the test, Reynolds number is about 20 between dendrites arms, increases to about 420 around the solidification front limit, and reach a maximal value of about 1150 on the viewing area of microscale images. In the three areas, the Reynolds number is pretty low seeming to indicate that the flow is laminar at the trailing edge of the weld pool.

4. DISCUSSION

The combination of the observations at macroscale and at microscale gives access to a map of the fluid flows in the whole weld pool. Figure 5 shows on the two sides the suggested fluid flow mapping. On the top side (Fig. 5a), the Marangoni effect, which is commonly the predominant force generating fluid flow in welding, drives the liquid from the hottest area (under the arc) to the edges of the weld pool, that are colder. Then, the liquid is pushed from the fusion line to the trailing edge by flowing along the solidification front. The flow is then separated in three components: the first one returns to the weld pool centre on the top side, leading to rotations of the two oxides clusters, the second one goes through the thickness to the back side of the weld pool in the liquid area, and the third goes through the thickness to the back side of the weld pool in the semi-solid area. On the back side of the weld pool (Fig. 5b), the liquid

coming from the semi-solid area and its vicinity goes through the rear of the weld pool to reach the centre of it. The flow produces the rotations of the oxides and goes back to the top side.

The thermal Péclet number ($Pe_{th}=uL_c/\alpha$, with u the fluid flow velocity, L_c a characteristic length and α the thermal diffusivity), which represent the ratio between thermal convection and thermal conduction, calculated at the weld pool scale is between 50 and 100. These values and the fluid flow mapping (Fig. 5a) highlight the fact that the fluid flows in the weld pool are mainly responsible for the heat transfer from the front of the weld pool to the trailing edge. The heat transfer from the front to the trailing edge helps to homogenise the temperature and can be one of the causes of the characteristic shape of solidification front. It is illustrated on Figure 6a. The hot liquid flows on the top side to the trailing edge, retarding solidification and elongating the weld pool. By flowing through the semi-solid area from top side to back side, the liquid is cooled. The solidification is then less retarded in the back side, and the weld pool rear is less elongated

The fluid flow has not only an effect on heat transfer. As it is seen in lots of publications [4], [5], the solute concentration in the vicinity of the dendrites has an effect on the growth velocity. If the solute concentration is locally modified in the liquid near the dendritic surface, the solidification rate would be changed. In the case of this study, the fluid flow observed in the vicinity of dendrites arms and the deduced flow in the whole semi-solid region influences the solidification. The solutal Péclet number ($Pe_{th}=uL_c/D_l$, with u

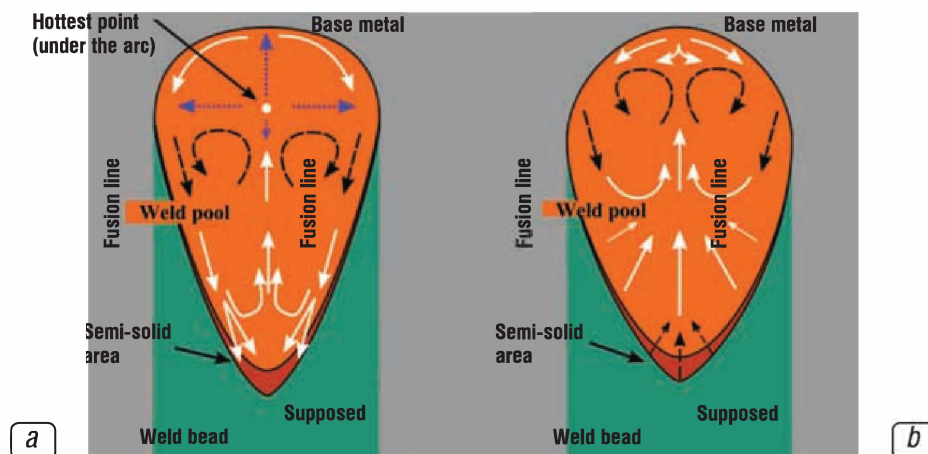


Fig. 5. fluid flow mapping (a) on the top side of the weld pool, and (b) on the back side of the weld pool. The fluid flows are coded by origin in three colours

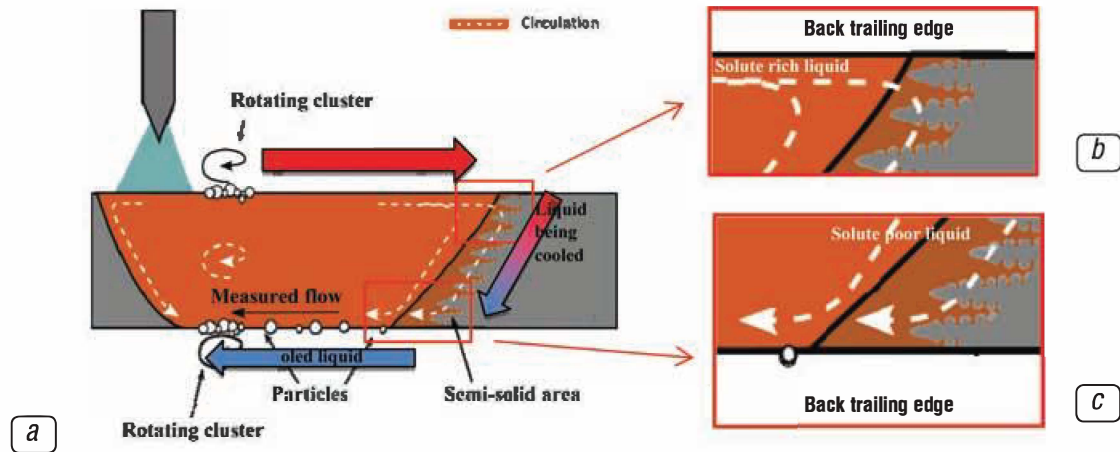


Fig. 6. Illustration of the effects of the fluid flows on the solidification front

the fluid flow velocity, L_c a characteristic length and D_l the diffusivity coefficient of the solute) calculated between dendrite is greater than one. Therefore, the convection leads the solute transfer in the liquid near dendrites and the fluid flow controls the solidification condition in the semi-solid area.

As the partition coefficient (ratio between solute concentration in solid and liquid phases) of the Cu_{30}Ni alloy is superior to 1, the liquid arriving from the liquid pool at the top trailing edge of the weld pool is solute rich (Fig. 6a). At the opposite, the liquid coming from the semi-solid area could be solute poor (Figure 6(b)), because the solute of the liquid flowing through the semi-solid area is absorbed by the dendrites during solidification. Consequently, between the top and the back side of the semi-solid area, the liquid could be more and more solute poor, decreasing the primary dendrite arms velocity and retarding the solidification on the back side. This phenomenon is not observed, that seems to indicate the effect of thermal convection is predominant at macroscale. However, the solute impoverishment can influence the size or the growth velocity of secondary dendrite arms. On microscale videos, no secondary dendrite arms have been observed and only very long primary dendrite arms have been observed. It can be caused by the solute poor liquid flowing between the dendrite arms, slowing down the growth of secondary arms.

5. CONCLUSION

The solidification during GTA welding has been investigated with the help of in-situ observations. The designed setup allows the observation

in the same time of the weld pool at macroscale on both sides in visible light and on the back side in infrared light, as well as at microscale with a high-speed camera.

Measurements have been extracted from the observation to access the parameters influencing solidification. A complete mapping of the fluid flows in the weld pool has been deduced from the different measurement at the two scales. The presence of fluid flow has been discovered in liquid channels between the primary dendrite arms in the semi-solid area.

Several hypotheses have been made on the influence of fluid flows on solidification. The fluid flow in the weld pool could extend the top side weld pool by retarding the solidification due to the arrival of hot liquid in the trailing edge. The fluid flow in the semi-solid area also changes the solidification conditions between top side and back side of the trailing edge.

REFERENCES

1. Hunziker O., Dye D., Reed R. On the formation of a centreline grain boundary during fusion welding // *Acta Mater.* — 2000, Nov. — Vol. 48, № 17. — P. 4191–4201.
2. Kou S. *Welding Metallurgy*, Second. John Wiley & Sons, Inc., 2003.
3. Kou S. Fluid flow and solidification in welding: three decades of fundamentals research at the university of Wisconsin // *Weld. J.* — 2012. — Vol. 91. — P. 287s–302s.
4. Boden S., Eckert S., Gerbeth G. Visualization of freckle formation induced by forced melt convection in solidifying GaIn alloys // *Mater. Lett.* — 2010, June. — Vol. 64, № 12. — P. 1340–1343.

5. *Gandin C.-A., Guillemot G., Appolaire B., Niane N.T.* Boundary layer correlation for dendrite tip growth with fluid flow // *Mater. Sci. Eng. A.* — 2003, Feb. — Vol. 342, № 1–2. — P. 44–50.
 6. *Bobadilla M., Lacaze J., Lesoult G.* Influence des conditions de solidification sur le déroulement de la solidification des aciers inoxydables austénitiques // *J. Cryst. Growth.* — 1988. — Vol. 89. — P. 531–544.
 7. *Bouissou P., Pelce P.* Effect of a forced flow on dendritic growth // *Phys. Rev. A.* — 1989. — Vol. 40, № 11. — P. 6673–6680.
 8. *Kurz W., Fisher K.* Fundamentals of solidification, Third rev. *Trans Tech Publications Ltd*, 1992.
 9. *Zhao C.X., Steijn V. van, Richardson I.M., Kleijn C.R., Kenjeres S., Saldi Z.* Unsteady interfacial phenomena during inward weld pool flow with an active surface oxide // *Sci. Technol. Weld. Join.* — 2009. — Vol. 14, № 2. — P. 132–140.
 10. *Chiocca A., Soulié F., Deschaux-Beaume F., Bordreuil C.* In situ observations and measurements during solidification of CuNi weld pools // *Sci. Technol. Weld. Join.* — 2016, May. — Vol. 1718. — P. 7.
-
-